University of Alberta

A Molecular Dynamics Study of the Dissolution of Asphaltene Model Compounds in Supercritical Fluids

by

Ali Javaheri

A thesis submitted to the Faculty of Graduate Studies and Research
in partial fulfillment of the requirements for the degree of

Master of Science
in
Chemical Engineering

Chemical and Material Engineering

Spring 2011
Edmonton, Alberta

Examining Committee

Phillip Choi, Chemical and Materials Engineering

Zhenghe Xu, Chemical and Materials Engineering

Juliana Leung, Civil and Environmental Engineering

Abstract

The demand for a new solvent to treat oilsands was behind the purpose of this project; molecular dynamics simulation was used in this study. Supercritical water, supercritical carbon dioxide and other selected organic solvents in their supercritical state were studied. Meso-tetraphenyl porphyrin (H_2TPP) and Octaethyl porphyrin (H_2OEP) are the porphyrin model compounds and, 4'-Bis-(2-pyren-1-yl-ethyl)-[2, 2'] bipyridinyl (PBP) is the asphaltene model compound. A solubility parameter approach was used to infer the solubility of model compounds in the supercritical fluids. First, the solubility of water, carbon dioxide, 4 selected organic solvents, and the three model compounds were computed using molecular dynamics simulation and compared with experimental results. The computed solubility parameters showed that the model compounds would dissolve in supercritical water (22.5 MPa and 645-655 K) but exhibited no solubility in supercritical carbon dioxide.

Acknowledgments

I am indebted to one of my co-supervisors, Dr. Phillip Choi, whose patience and kindness, as well as his academic experience, had been invaluable to the preparation of this thesis. I appreciate his creative insights and ideas, which provided a great learning experience during this research.

Special thanks to my other co-supervisor Dr. Xu for his insightful and helpful comments and for making clear to me various issues.

I would also like to thank the Centre for Oilsands Innovation (COSI) for supporting my work, graphically.

My deepest gratitude goes to my family for their love and support. I would like to thank them for being a great encouragement in my life.

Table of contents

Chapter 1 Introduction Page

1.1 Supercritical fluid extraction 1

1.2 The oilsands extraction process 3

1.3 Cohesive energy density 6

1.4 Use of the solubility parameter concept for supercritical fluids 7

1.5 Molecular simulation 9

1.6 Overview and scope of thesis 10

Chapter 2 Asphaltenes

2.1 Asphaltenes 11

2.2 Asphaltene model compounds 13

Chapter 3 Molecular Dynamics Simulation

3.1 Introduction 16

3.2 Formulation 17

3.3 Atomistic model 21

3.4 Ensembles in MD 23

3.5 Periodic conditions 24

3.6 Force fields 25

3.7 Minimization methods 26

3.8 Water models 27

3.9 Simulation procedure 29

Chapter 4 Results and Discussions

4.1 Testing the force field with supercritical data 30

4.2 System size dependence of errors 33

4.3 Solubility parameters of selected organic solvents at room temperature 34

4.4 Solubility parameters of selected organic solvents in the supercritical region 36

4.5 Solubility Parameter of Model Compounds at Ambient Temperature 37

4.6 Solubility Parameters of Model Compounds at Supercritical Regions 38

4.7 Mixtures 40

Chapter 5 Conclusion and Future Work

5.1 Conclusion 43

5.2 Future Work 44

List of Figures

Page

Figure 2-1 Structures of H_2TPP, H_2OEP and a model asphaltene compound PBP 15

Figure 3-1 schematic view of a simulation cell subjected to periodic boundary condition 25

Figure 4-1 Pressure results, MD simulation vs. experiment 31

Figure 4-2 Pressure results for carbon dioxide, experiment vs. MD simulation at 0.004 (mol/cm^3) 32

Figure 4-3 Pressure results for carbon dioxide, experiment vs. MD simulation at 0.001 (mol/cm^3) 32

Figure 4-4 Optimum cell size for a sample simulation at 25 ^{0}C and 0.001 GPa, obtained from two initial configurations for each cell size 33

Figure 4-5 Solubility parameters for different solvents 35

Figure 4-6 Solubility parameters for different solvents at SC region 36

Figure 4-7 Solubility parameters for model compounds, Experiment vs. MD 38

Figure 4-8 Solubility parameters of model compounds and supercritical fluids in SC regions 39

Figure 4-9 Mixture of four H_2 OEP and one hundred CO_2 molecules in the SC region 41

Figure 4-10 Mixture of four H_2 OEP and one hundred CO_2 molecules in the SC region

Figure 4-11 Mixture of four H_2 OEP and one hundred H_2O molecules 41

in the SC region 42

Figure 4-12 Mixture of four H_2 OEP and one hundred H_2O molecules

in the SC region 42

List of Tables

Page

Table 1-1 Critical properties of carbon dioxide and water 1

Table 3-1 Water models and properties 28

Table 4-1 Calculated and experimental solubility parameters of four organic solvents and water at ambient temperature 35

Table 4-2 Solubility parameters ($MPa^{0.5}$) for Model Compounds at 20 ^{0}C 37

Chapter 1

Introduction

1.1 Supercritical Fluid Extraction

Depending on the temperature and pressure, a substance can exist in one of the four phases (solid, liquid, gas and supercritical phases) or in co-existing phases. When the temperature and pressure are above the critical temperature and critical pressure of a substance, usually referred to as vapor-liquid critical point, it is in the supercritical phase. At the critical point, the physical properties of vapor and liquid become identical. It is worth noting that the most common supercritical fluids used in industry are carbon dioxide and water.

The critical properties of CO_2 and H_2O are shown in the following table.

Table 1-1 Critical properties of carbon dioxide and water

Substance	Molecular weight (g/mol)	Critical temperature (K)	Critical pressure (MPa)	Critical density (g/cm^3)
CO_2	44.01	304.1	7.38	0.469
H_2O	18.015	647.096	22.064	0.322

Supercritical fluids (SCFs) are ideal candidates to be used as solvents in certain extraction processes because such fluids combine properties of both gases and liquids

which greatly improve their solvent capabilities [1]. Near the critical point, properties of supercritical fluids are strongly dependant on temperature and pressure [2]. The benefits of these characteristics have been well documented and they include: increased solubility reduced solvent to feed ratios, easier solvent recovery, reduced mass transfer resistance, lower operating temperatures resulting in lower energy requirements and finally, and since the solubility power of supercritical fluids change by temperature, permits the synthesis of temperature sensitive products [2-5].

The benefits of employing supercritical fluids for processing hydrocarbon mixtures are evident in the success of the ROSE (Residuum Oil Supercritical Extraction) process and propane deasphalting [6]. These processes rely on the solvent behavior of fluids near their critical points to remove asphaltenes from streams such as lube oil feeds. Research is also being conducted in an attempt to apply supercritical fluids to other areas of the fossil fuel industry; these include areas such as: processing and liquefaction of coal [7, 8], extraction of oil from oil shales [9-11], oilshale is an organic-rich fine-grained sedimentary rock, which contains significant amounts of kerogen (a solid mixture of organic chemical compounds) from which liquid hydrocarbons can be extracted fractionation of crude oils, bitumen and wax-bearing residue [12-15], analytical tools for the characterization of bitumen's and heavy hydrocarbon mixtures [16] and in the in situ production of heavy oils [17], In situ refers to recovery techniques which apply heat or solvents to heavy oil or bitumen reservoirs beneath the earth. There are several varieties of in situ technique, but the ones which work best in the oil sands use heat.

Supercritical water behaves like an organic liquid with high solubility of organic compounds in it which are otherwise insoluble in ambient water [14]. This has generated

a lot of interest because of its tremendous potential as an environmentally benign solvent for the oxidative destruction of hazardous wastes in chemical industries. Moreover, supercritical water can be used to transform organic waste partially into light feed stocks [16].

Supercritical water is a dense steam and can be miscible with light gases and hydrocarbons to form a homogeneous phase by the proper choice of temperature and pressure. R-O-R and R-C=O bonds, such as those found in ethers and esters, and the aliphatic C-H and C-S bonds are easily broken in supercritical water [1]. The thermal reaction of heavy oil is of considerable practical interest and it has been studied in supercritical water. Under supercritical conditions, two major reactions occur: oxidation and hydrolysis [5]. Owing to these reactions, tar can be decomposed successfully into useful chemical compounds in supercritical water [10, 11]. In one research, oil shale was treated with supercritical water and resulted in a higher conversion and a higher oil recovery than that obtained from toluene extraction. Supercritical water also yields more facile decomposition of the polar components in oil shale compared to supercritical toluene [13]. Supercritical carbon dioxide (*sc*-CO_2) could be viewed as the ideal chemical processing solvent as well; it is cheap, nontoxic, volatile, inert, non-flammable, and recycable.

1.2 The Oilsands Extraction Process

Oilsands are deposits of organic/inorganic mixtures which basically consist of sand, water, and a black viscous tar-like material called bitumen. Due to the vast global demand of energy during the last few decades and the growth of oil prices as an

aftermath, extraction of oil or bitumen from oilsands has drawn the attention of a number of oil companies. Oilsands is known as unconventional oil since techniques different from the ones used for traditional oil wells are used to extract petroleum. A typical commercially viable oilsands deposit contains 9%-13% bitumen, 3%-7% water, and 80%-85% mineral solids. Of the solids 15%-30% are fine particles, predominantly clays, less than 44 μm in diameter [18]. Currently, lots of countries across the globe have deposits of oilsands such as Canada, Venezuela, parts of Russia and Africa. But the main resources reside in Canada and Venezuela in which their current reserves equal all discovered conventional oil reserves [19]. Oil sands may represent as much as two-thirds of the world's total petroleum resource, with at least 1.7 trillion barrels (270×10^9 m^3) in the Canadian Athabasca Oil Sands and perhaps 235 billion barrels (37×10^9 m^3) of extra heavy crude in the Venezuelan Orinoco Oil Sands [19]. As a result of the development of Canadian oil sands reserves, 44% of Canadian oil production in 2007 was from oil sands, with an additional 18% being heavy oil, while light oil and condensate have declined to 38% of the total [20]. In 2006, bitumen production averaged 1.25 million barrels per day (200,000 m^3/d) through 81 oil sands projects, representing 47% of total Canadian petroleum production. This proportion is expected to increase in the coming decades as bitumen production grows while conventional oil production declines. In the Athabasca region, the oilsands is covered with layers of rock and soil which is called overburden. This overburden is removed with surface mining to reach the oilsand, rather than with underground mining in which a tunnel is usually dogged to reach required mineral and the rest of the soil would be left at the place. This method has been used on a commercial scale since 1967, there are several types of mining: strip mining, open pit mining,

mountain dredging and high wall mining top removal. It is estimated that approximately 80% of the Alberta oil sands and nearly all of Venezuelan oilsands are too far below the surface to use open-pit mining. Several in-situ techniques have been developed to extract this oil [20] and they are:

1. Steam assisted gravity drainage (SAGD)

2. Vapor Extraction Process (VAPEX)

3. Toe to Heel Air Injection (THAI)

4. Cold flow

As any other major projects on this planet, oilsands projects have their own environmental impacts as well. Many non-governmental organizations (NGOs) have taken this issue seriously during the past years and have pressured the government to seize or control the production of oil from oilsands. The main environmental impacts of oilsands can be categorized in 4 parts:

1. Land

2. Water

3. Air

4. Tailings

One of the major problems that remain to be solved is the economical and environmental acceptable treatment and ultimate disposal of tailings that result from the hot water separation process. A considerable amount of water is used for oil sands operations –

Greenpeace gives the number as 349 million cubic meters per year, twice the amount of water used by the city of Calgary. Due to the environmental drawbacks of the hot water extraction process, oil companies have been seeking new extraction solvents to resolve the issue. The search for nontoxic, recycable and environmentally benign solvents for use as extraction medium is imperative. In this context, supercritical fluids have drawn some attention.

1.3 Cohesive Energy Density

The cohesive energy density is the amount of energy needed to completely vaporize a unit volume of substance in their liquid state to the ideal gas state. In other words, it is equal to the internal energy change of vaporization (ΔU_v) divided by the molar volume (V_m) of the liquid. Based on the idea of like dissolves like, in order for a substance to dissolve into another substance, they should exhibit comparable intermolecular interactions (i.e., comparable cohesive energy density). Hildebrand defined the square root of the cohesive energy density as the "Hildebrand solubility parameter" and suggested that materials with similar solubility parameters will be able to interact with each other, resulting in solvation, miscibility or swelling [21].

$$\delta = \sqrt{\frac{\Delta U_v}{V_m}} \tag{1.1}$$

1.3.1 Regular Solution Theory

In order to model the solubility of a solute (2) in a solvent (1), it is necessary to have an estimate for the mole fraction of the solute (x_2) in the liquid phase. According to the regular solution theory, we have:

$$\ln(\frac{1}{x_2}) = \frac{V_2^l(\delta_1 - \delta_2)^2 \varphi_1^2}{RT} \quad (1.2)$$

where V_2^l is the molar volume of the sub cooled liquid solute at temperature T; δ_i is the solubility parameter of component i; R is the ideal gas constant (8.314 J/mol·K) and φ_1 is the volume fraction of the solvent.

1.4 Use of the Solubility Parameter Concept for Supercritical Fluids

There are only a few methods to correlate solubility of substances in supercritical fluids.

1) Empirical or cubic equations of state (EoS) for mixtures such as those of Redlich and Kwong and Peng Robinson [2] (binary interaction parameters are needed).
2) Correlating solubility parameter data such as that of Chrastil [22].

To our knowledge, there is only one method available for the prior prediction of solubility's in SCF, using pure component data and a correlation for binary mixtures. Lutge et al. [23] called attention to the method of Wong et al. [24]. As the only truly predictive method, Johnston et al. [25] later reviewed it from a different perspective. Brennecke and Eckert [26], in an excellent phase-equilibrium review, discussed solubility

of solids in SCF based on cubic and perturbed-sphere EOSs, in terms of hard-sphere van der Waals (HSVDW) model. However, for engineering purposes or in exploratory work, the accuracy requirement can be relaxed. This is because approximate data are often an acceptable basis for certain early stage design decisions. For example, in the case where information is needed to proceed pilot-plant runs, Lutge[27] has shown that estimated solubility is sufficient for judging a SCF soil clean-up process using a reduced set of experimental data.

Solubility parameters (SPs) play a significant role in the indication of the solubility of solutes in solvents. Various applications of SPs relating to supercritical fluids have been reported in literature. The use of SPs for supercritical fluid chromatography (SCC) was supported by Giddings et al. [28, 29]. The role of supercritical fluid extraction (SCE) in the field of SCC was discussed by King [30]. Riekkola and Mannien [31] reviewed SCE as another sample preparation method and reported on the effect of SPs on solubility's in SCFs. Ikushima et al. [32] applied modified SPs to correlate such solubility observation. Allada [33] in a paper entitled "Solubility parameters of Supercritical Fluids", addressed this subject directly. Panayiotou [34] more recently revisited the SPs using equations of state for their estimation and included applications to SCFs.

The common formula for estimation of solubility parameters is equation (1.1). However, for SCFs, such a definition is meaningless as internal energy change of vaporization is not relevant to supercritical fluids. Giddings et al. [28] suggested this correlation:

$$\delta = 1.25 P_c^{0.5} \left(\frac{\rho_r SCF}{\rho_r liq}\right) \qquad (1.3)$$

where P_c is the critical pressure and $\rho_r SCF$ is the reduced density of the supercritical fluid. There are other correlations derived from other EOSs namely Redlich Kwong equation of state in literature as well as Goldman et al. [35].

1.5 Molecular Simulation

Since it is expensive to run supercritical fluid experiments, in this thesis we explore the dissolution of asphaltene model compounds in selected substances (carbon dioxide, water and some organic solvents) in their supercritical state through molecular dynamics (MD) simulation. The reason for choosing asphaltene model compounds is due to the fact that the molecular structures of bitumen or asphaltene, a major component of bitumen, are not known. Asphaltene structures will be discussed in the next chapter. There are numerous reports in literature using molecular simulation to explore solubility characteristics of supercritical fluids. Li et al. [36] calculated the miscibility properties (i.e., solubility parameters) of asphaltene model compound using Monte Carlo simulations. The aggregation of asphaltene molecules was studied using molecular modeling techniques by E.Rogel [37]. In particular, the solubility parameters of two different asphaltene molecules and their aggregates were calculated. The results show a decrease in this parameter with increasing aggregation state, in agreement with experimental evidence [38]. In another research, the influences of six different solvents (nitrobenzene, quinoline, pyridine, 1-methylnaphthalene, dibromomethane and benzene) on the aggregation process of asphaltene molecules were investigated at normal and elevated temperatures. According to the analyses of structures and energy, the main intermolecular interaction for the asphaltene aggregate was determined, and the influencing mechanism for the

asphaltene stability in different solvents was discussed at 300 K and 573 K. It was found that van-der-Waals (VDW) interaction plays an important role in the stability of the asphaltene aggregate [39] .All of these simulations have focused on the aggregation of asphaltenes at ambient conditions. In this thesis, we focus on the aggregation of asphaltene model compounds in supercritical fluids and also the use of solubility parameters in the supercritical region to predict the dissolution of model compounds.

1.6 Overview and Scope of the Thesis

In Chapter 2, we will discuss properties of asphaltenes and the type of model compounds we will use for the simulations. In Chapter 3, we will give a brief discussion about molecular dynamics simulation and will discuss the simulation parameters and the water model we used for the simulation.

In Chapter 4, we will present the results of the simulations for the pure solvents and the asphaltene model compounds and compare them with experimental data. Solubility parameter approach was used to analyze the miscibility of model compounds and supercritical fluids in the supercritical region, aggregation of model compounds in supercritical region was also studied qualitatively to back the quantitative data gained via solubility approach. In Chapter 5, we will give a few concluding remarks, a list of future work and give out suggestions for practice.

Chapter 2

Asphaltenes

2.1 Asphaltenes

Dilution of Alberta bitumens in n-pentane or n-heptane precipitates 10-20% of brown/black solid precipitate. This solid fraction is called “asphaltenes”. Obviously, there exists no unique chemical structure for asphaltenes. They contain molecules that do not dissolve in alkanes.

Asphaltenes are molecular substances that are found in crude oil, along with resins, aromatic hydrocarbons, and alkanes (i.e., saturated hydrocarbons) [40]. However, the most commonly used definition for asphaltenes is that they are substances that are insoluble in n-heptane (C_7H_{16}) at a dilution of 40 parts alkane to 1 part crude oil and are soluble in toluene ($C_6H_5CH_3$). Of course, the temperature at which the dissolution occurs and the time of mixing is all important factors in this definition.

From a chemical element perspective, asphaltenes consist primarily of carbon, hydrogen, nitrogen, oxygen, and sulfur, as well as trace amounts of vanadium and nickel. The C: H ratio is approximately 1:1.2, depending on the asphaltene source. Asphaltenes have been shown to have a distribution of molecular masses in the range of 400 g/mol to 1500 g/mol with a most probable mass around 750 g/mol [41]. Asphaltenes had been thought to be held in oil by resins (similar structure and chemistry, but smaller molecules).

Asphaltene deposition occurs on well site, in wells, tubing and piping or in any stage of the refining process [42]. The spontaneous emulsification due to asphaltenes happens usually during the production of the crude oil. These emulsions must be broken by chemical or physical methods before the treatment of oil [43]. Reservoir damage, decrease in production, equipment damage and large control costs are some of the consequences of these problems. The asphaltene fraction consists of many different molecules of different molecular weights and polarity but having the same solubility properties in the oil or precipitation solvent [44]. The molecular weights of this fraction as determined by vapor pressure osmometry vary considerably and are dependent upon the nature of the solvent as well as the temperature used [45].

It is well known that the asphaltenes are highly polydisperse molecules and in consequence the use of a mean structure may not be a good approximation. However, the asphaltenes do not crystallize and can't be separated into individual components making the fine chemical analysis essentially impossible [42]. For this reason, whatever its limitations, the average molecule approach is widely used to represent asphaltene fractions [46].

A more realistic modeling is to use a distribution of molecules that take into account the polydispersity of this fraction. Molecular weight and heteroatom distributions for asphaltene fractions are reported in literature [47, 48]. However, molecular weight distributions must be interpreted with caution due to the tendency of asphaltenes to form aggregates. Additionally, determination of heteroatom distributions requires the use of techniques that are not generally available [46]. One important aspect in the modeling of a realistic asphaltene distribution is the selection of functional groups that contain

heteroatom. Some results [49] indicate that the behavior of asphaltenes is strongly dependent on the type and proportion of the different functionalities and also it is well known that the heteroatomic functional groups have a big influence on the solubility parameter [50]. Unfortunately, even though it is possible to identify the functional groups in the asphaltene fraction, this characterization is expensive and time consuming and the data are not generally available [46].

Asphaltene precipitation basically happens in three steps:

1. the molecules stick together and form dimmers, timers and other aggregates;
2. the aggregates come together to form micelle structures;
3. the attraction force between micelles cause the asphalte
4. ne to precipitate as a whole;

A number of theoretical models have been applied to study the precipitation phenomenon of asphaltenes. Flory-Huggins regular solution based models and others that use equations of state are examples of the thermodynamic approaches used for asphaltenes. They assume that asphaltenes are solvated in the crude oil and precipitate whenever their solubility drops below a certain threshold [51]. Another approach is to consider asphaltenes as colloidal systems [52] stabilized by resins.

2.2 Asphaltene Model Compounds

Several structures have been proposed for model compounds by different researchers such as: Andersen and Speight [51], Brandt et al. [53], Rogel [54], Murgich et al. [55]

and Zajac et al. [56]. Although these models have led to significant insight into the chemistry of asphaltenes, many aspects still remain to be established, such as the discrepancies by a factor of 10 on molecular weights.

In this project, we used three model compounds – two porphyrin and one asphaltene model compound. Meso-tetraphenyl porphyrin (H_2TPP) and Octaethyl porphyrin (H_2OEP) are the porphyrin models and, 4'-Bis-(2-pyren-1-yl-ethyl)-[2, 2'] bipyridinyl (PBP) is the asphaltene model compound. The structures of these three compounds are presented in the figure below:

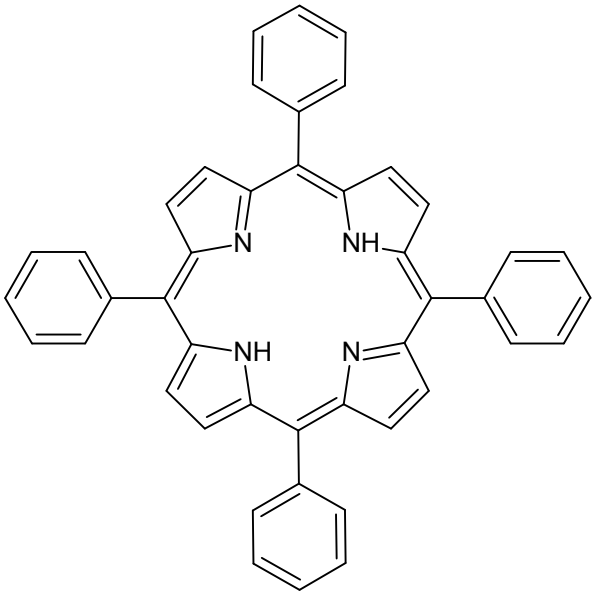

Meso-tetraphenyl porphyrin (H_2TPP)

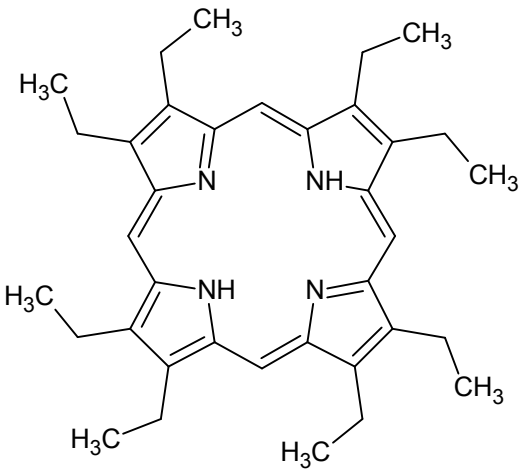

Octaethyl porphyrin (H_2OEP)

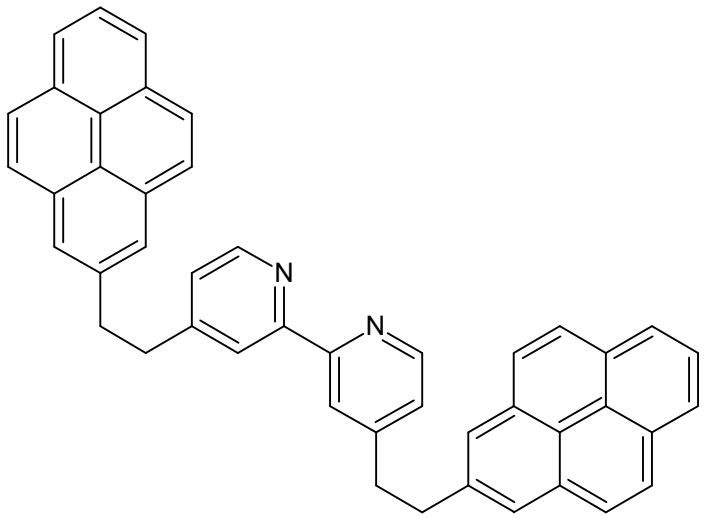

(PBP)

Figure 2-1 Structures of H_2TPP, H_2OEP and a model asphaltene compound PBP.

Chapter 3

Molecular Dynamics Simulation

3.1 Introduction

Molecular dynamics (MD) simulation has been used for the investigation of various phenomena for a long time, and it is almost 40 years since the first report of a MD simulation of condensed matter [57]. The "mechanical" molecular model was developed out of a necessity to explain molecular structures and properties. If one is interested in thermal properties, it is possibly the most understandable way of using a computer to produce a phase-space trajectory for an assembly of interacting atoms, and amounts simply to the stepwise integration of Newton's equations of motion from a totally specified starting point. If a system follows the ergodic principle, we then have the guarantee that time averages over these phase-space trajectories are equivalent to ensemble averages, and we have, therefore, every macroscopic property that can be associated with atomic motions through statistical mechanics [58]. These include time dependent quantities such as transport coefficients, which clearly engage the dynamical motion of the atoms and their correlations in time [59, 60]. Also, MD can be used to investigate relaxation towards equilibrium, and as such is a way to look at the configuration-space of a system so as to find the local minima. The techniques of MD and the many algorithmic innovations which have been made are described in the books by Allen and Tildesley [61] and Haile [62].

Molecular mechanics methods are based on the following principles:

- Nuclei and electrons are lumped into atom-like particles.
- Atom-like particles are spherical (radii obtained from measurements or theory) and have a net charge (obtained from theory).
- Interactions are based on springs and classical potentials.
- Interactions must be preassigned to specific sets of atoms.

Interactions determine the spatial distribution of atom-like particles and their energies.

3.2 Formulation

Molecular dynamics alter the intermolecular degrees of freedom in a step-wise mode, similar to energy minimization. The individual steps in energy minimization are simply directed at establishing a down-hill track to a minimum. The steps in molecular dynamics, on the other hand, significantly represent the changes in atomic position and velocity, r_i and v_i, over time.

Newton's equation is used in the molecular dynamics formalism to simulate atomic motion:

$$\overline{F_i} = m_i \overline{a}_1 \qquad (3.1)$$

The rate and direction of motion (velocity) are governed by the forces that the atoms of the system apply on each other as described by Newton's equation. In practice, the atoms are assigned initial velocities that match the Maxwell-Boltzmann distribution, which in turn, is dictated by the required simulation temperature. This is carried out by gradually

"heating" the system (primarily at absolute zero) and then allowing the energy to come to equilibrium among the constituent atoms. The basic ingredients of molecular dynamics are the calculation of the force on each atom, and from that information, the position of each atom all through a specified period of time (normally on the order of picoseconds = 10^{-12} seconds).

The force on an atom can be calculated from the change in energy between its current position and its position a small distance away. This can be recognized as the derivative of the energy with respect to the change in the atom's position:

$$-\frac{dV}{dr_i} = F_1 \tag{3.2}$$

Energies can be calculated using either molecular mechanics or quantum mechanics methods. Molecular mechanics energies are limited to applications that do not involve severe changes in electronic structure such as bond making/breaking. Quantum mechanical energies can be used to study dynamic processes involving chemical changes. Knowledge of the atomic forces and masses can then be used to solve for the positions of each atom along a series of very small time steps (on the order of femtoseconds = 10^{-15} seconds). The resulting series of snapshots of structural changes over time are called a trajectory. The use of this method to compute trajectories can be more simply seen when Newton's equation is expressed in the following form:

$$-\frac{dV}{dr_i} = m_i \frac{d^2 r_1}{dt^2} \tag{3.3}$$

In practice, trajectories are not directly obtained from Newton's equation due to the lack of an analytical solution. First, the atomic accelerations are computed from the forces and masses. The velocities are next calculated from the accelerations based on the following relationship:

$$a_i = \frac{dv_i}{dt} \tag{3.4}$$

Finally, the positions are calculated from the velocities:

$$v_i = \frac{dr_i}{dt} \tag{3.5}$$

The slow solution of the equations of motion using a finite difference method is performed by the use of an integration algorithm. One widespread algorithm is the Verlet algorithm [64]. This is derived from a Taylor expansion of the positions about time, t:

$$r(t+\delta t) = r(t) + v(t)\delta t + \tfrac{1}{2} a(t)\delta t^2 \tag{3.6}$$

$$r(t-\delta t) = r(t) - v(t)\delta t + \tfrac{1}{2} a(t)\delta t^2 \tag{3.7}$$

By adding the above equations, lead to:

$$r(t+\delta t) = 2r(t) - r(t-\delta t) + a(t)\delta t^2 \tag{3.8}$$

Velocities can also be calculated from:

$$v(t) = \frac{r(t+\delta t) - r(t-\delta t)}{2\delta t} \tag{3.9}$$

There are many modifications to the Verlet method to increase its efficiency and get more precise velocities.

A trajectory between two states can be subdivided into a series of sub-states separated by a small time step, " δt " (e.g. 1 femtosecond):

$$State1 - - - - - - - - - - - - - - - - - > State2$$

$$r_i^1 - - - > r_i^{1a} - - - > - - - > - - - > - - - > r_1^2$$

t t+ δt trajectory

The initial atomic positions at time "t" are used to predict the atomic positions at time "t + δt ". The positions at "t + δt "are used to predict the positions at "t + 2* δt ", and so on.

The "leapfrog" method is a common numerical approach to calculating trajectories based on Newton's equation. The method derives its name from the fact that the velocity and position information in sequence interchange at 1/2 time step intervals. Molecular dynamics have no defined point of break other than the amount of time that can be basically covered. Unfortunately, the current picoseconds order of magnitude limit is often not long enough to follow many kinds of state-to-state transformations, such as large conformational transitions in proteins.

In this work,a commercial software, Material Studio, was used to carry out all MD simulations.

3.3 Atomistic Models

Atomistic models are the most comprehensive models used in simulation. Here molecules are represented as a number of atomic sites associated by chemical bonds. The interaction between these atoms is described by a potential, commonly known as a *force field*, which includes terms to clarify bond stretches, bond angle bends, torsional rotations and non-bonded interactions. Additional terms to describe coupling between different distortions (e.g. coupling between a torsional rotation and a bond stretch) or other interactions such as hydrogen bonding that may also be present. The accurate form of each term can change from force field to force field. Bond stretches are usually described by a Taylor expansion of the energy about the equilibrium bond length l :

$$V(l) = V(l_0) + \frac{1}{2}(\frac{\partial^2 V}{\partial l^2})_{l=l_0}(l-l_0)^2 + \frac{1}{6}(\frac{\partial^3 V}{\partial l^3})_{l=l_0}(l-l_0)^3 + ... \qquad (3.10)$$

where l is the bond length.

The linear term in the above expansion is dropped as the force $(-\frac{\partial V}{\partial l})$ is zero at equilibrium. As bond stretches are of a large energy, this is often simplified at the quadratic term:

$$\Delta V(l) = \frac{1}{2}k_1(l-l_0)^2 \qquad (3.11)$$

Where ΔV (l) =V (l) -V (l_0) and $k_1=(\frac{\partial V}{\partial l^2})_{l=l_0}$. Similar terms are used for bond angle bending. Torsional rotations are modeled by a Fourier series:

$$V(\tau)=\frac{1}{2}V_1(1+\cos\tau)+\frac{1}{2}V_2(1-\cos 2\tau)+\frac{1}{2}V_3(1+\cos 3\tau) \quad (3.12)$$

where V_i are the torsional force constants. The non-bonded interactions are usually separated into Van der Waals and electrostatic interactions. The electrostatic interaction is modeled by point charges on the atoms interacting through Coulomb's law

$$V=\frac{1}{4\pi\varepsilon_0}\frac{q_i q_j}{r_{ij}} \quad (3.13)$$

where q_i, q_j are the point charges, r_{ij} is the distance between the charges and ε_0 is the permittivity of free space. For more sensible models of particle interactions, the forces vary smoothly as a function of position. Under the influence of a continuous potential the motions of all the particles become joined together, giving rise to a many body problem that cannot be solved analytically. Thus, a numerical approach, the *finite difference* method is used to solve the equations of motion. The general idea of the *finite difference* approach is that time can be broken down into a series of discrete steps of length δt. Given the molecular positions and velocities at a time, t, we attempt to find these at a later time t+δt with sufficient accuracy. Then, we can attempt to use these new positions and velocities to calculate positions and velocities at time t+2δt Thus the equations of motion are solved on a step-by-step basis.

3.4 Ensembles in MD

As the above equations produce trajectories with constant energy (within computer accuracy), it means that MD produces the micro canonical (NVE) ensemble. However, it is often of more interest to carry out simulations in other ensembles, commonly the canonical (constant temperature NVT) ensemble or the isothermal-isobaric (NPT) ensemble. To do this, it requires modifications to the standard equations of motion. In this work, we used NVT ensemble so we just focus on this one. Simulations at constant temperature are important for studying the performance of systems at different temperatures. There have been a number of different approaches for performing constant temperature (NVT) MD. As the temperature of a system is associated with the average kinetic energy of the particles, the temperature can be controlled by scaling the velocities, i.e. at each time step the velocities are scaled according to V=χV0 One such thermostat in this spirit is the Berensden thermostat [62] . Here the velocity rescaling parameter, χ, is given by

$$\chi = \left[1 + \frac{\delta t}{\tau}\left(\frac{T}{T_0} - 1\right)\right] \tag{3.14}$$

where δt is the time step, T, is the current temperature, T_0 is the set temperature, and τ is a time constant. A different method, like velocity rescaling, is to limit the velocities by a Gaussian constraint method [65]. Alternatively, the temperature can be held constant by a heat bath. In this method, the velocity of an arbitrarily selected particle is replaced by one selected from the Maxwell-Boltzmann distribution. This is correspondent to a collision with a particle in a made-up heat bath. A final possibility is the extended system method.

In this method, the system is assumed to be in contact with a heat bath. However, in this case the interaction between the simulated system and the heat bath is modeled by an interchange of energy between them. The equations of motion for this thermostat are

$$\dot{r} = \frac{p}{m} \tag{3.15}$$

$$\dot{p} = f - \zeta p \tag{3.16}$$

$$\zeta = \frac{g k_B T_0}{Q}\left(\frac{T}{T_0} - 1\right) \tag{3.17}$$

where ζ is a friction coefficient, g is the number of degrees of freedom, and Q is the thermal inertia coefficient, which describes the rate of energy exchange among the system and the heat bath.

3.5 Periodic Boundary Conditions

Computer simulations using atomistic models are usually performed on small systems, usually on the order of a few hundred molecules. For a simple cubic lattice, containing 1,000 molecules, around 50% of them lie on the surface. These molecules would experience forces different from other molecules. To resolve this issue, it is common to call up periodic boundary conditions. Here, the system is surrounded by an unlimited number of alike systems. During the simulation the molecules in each of the boxes move in the same way. Therefore, if a molecule leaves the simulation box at one side, an equal molecule enters the box at the other.

Here, we only consider interactions between each molecule and the closest periodic images of its neighbors. Short ranged forces are often truncated to raise computational efficiency. For reliability, this cut-off distance must be less than or equal to half the box length. Periodic boundary conditions can sometimes have an effect on the system under consideration. However, they have little effect on equilibrium properties. The most frequently formed simulation cell is cubic. It is also doable to use cells of other shapes, such as the rhombic or dodecahedron. For studying surfaces, it is common to keep periodicity in two dimensions, while discarding it in the direction perpendicular to the surface.

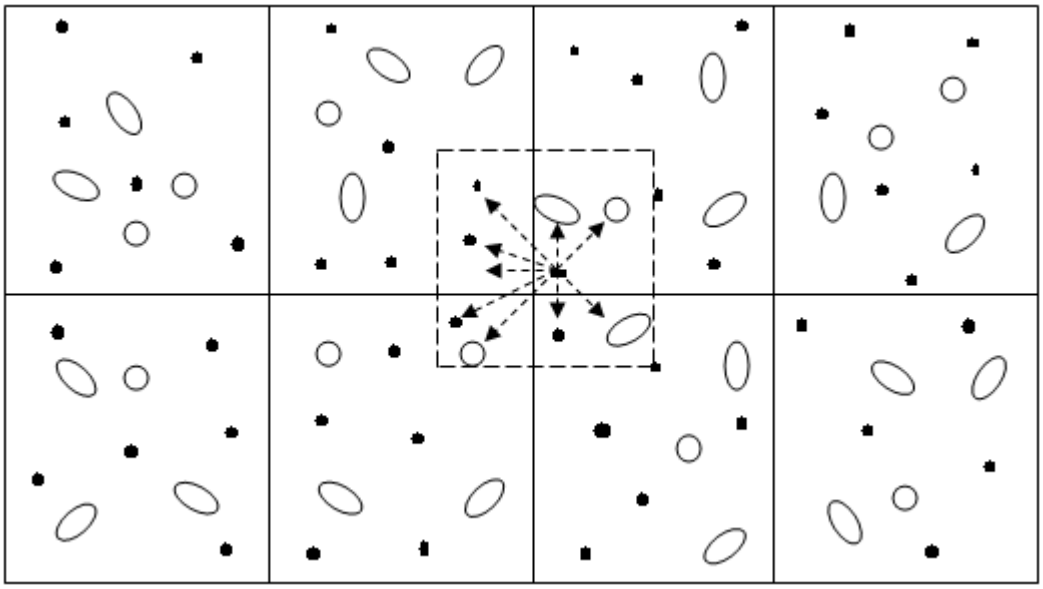

Figure 3-1 A schematic view of a simulation cell subjected to periodic boundary condition.

3.6 Force Fields

The basis of atomistic simulation is the potential, often called a *force field*. Using a force field, the energy of the molecule and the forces on its atoms can be calculated from atomic positions. There are many diverse force fields which use different forms for a

variety of interactions within and between molecules. The specific form of a force field depends on the precision required for its intended goal. Force field parameters can be found from either experimental or theoretical data. An important element for both the force field form and the force field parameters is that those for a particular atom or group of atoms should be the same for different molecules, i.e. they should be *transferable*. Without this property a different force field would have to be made for each different molecule. The COMPASS force field is used throughout the simulations [62]. COMPASS is the first ab initio-based force field to have been parameterized using extensive data for molecules in the condensed phase. This explains why COMPASS is able to make accurate predictions of structural, conformational, vibrational, cohesive, and thermophysical properties for a broad range of compounds, both in isolation and in condensed phases.

3.7 Minimization Methods

There are several methods to minimize the energy of a molecular system. All these methods need the ability to calculate the value of the function given a particular set of parameters used for the model. There are methods which require only the function values. Some methods require gradient of the function as well. These methods, as a class, are called Gradient Descent methods.

The method of minimization which uses the gradient and all of the second derivative (or bending) information is called the ``Full-Matrix" method. The Full-Matrix method is fairly robust but the requirements of memory and computations for its execution are

computationally very demanding. Also, this algorithm can only be used when the model is very close to the minimum. For proteins, it has only been applied to cases where the molecule is small (< 1,000 atoms), which requires high resolution and have formerly been thoroughly refined with gradient descent methods.

There are three algorithms used in the discover minimizer module in the Materials Studio:

1) steepest descent
2) conjugate gradient
3) Newton method

We used the conjugate gradient method for minimizing the energy of the system [62].

3.8 Water Models

Since supercritical water was studied, we describe various water models in this section as the type of water model used in the simulations can play a major role in the results. Some models show a lack of strength due to their sensitivity to the exact model parameters. [66] A number of these models use water molecules with a wider (more tetrahedral) H-O-H angle and longer H-O bond length than those expected of gaseous or liquid water and this is significant in terms of modeling hydrogen bonding. A recent review yielded 46 distinct water models [67].

And Table 3-1 summarizes some of the most successful water models along with their relevant parameters.

Table 3-1 Water models and properties

MODEL	δ Å	ε KJ MOL^{-1}	L_1 Å	L_2 Å	Q_1 (E)	Q_2 (E)	Θ°	Φ°
SPC[68]	3.166	0.650	1.0000	-	+0.410	-0.8200	109.47	-
TIP3P[69]	3.15061	0.6364	0.9572	-	+0.4170	-0.8340	104.52	-
TIP4P[69]	3.15365	0.6480	0.9572	0.15	+0.5200	-1.0400	104.52	52.26
COS/G3[70]	3.17459	0.9445	1.0000	0.15	+0.450672	-0.901344	109.47	-
Six-site[71]	3.115_{OO} 0.673_{HH}	0.715_{OO} 0.115_{HH}	0.980	0.8892_{L} 0.230_{M}	+0.477	-0.044_{L} -0.866_{M}	108.00	111.00
QCT[72]	.140	0.753	0.9614	-	+0.6064	-1.2128	104.067	-

where σ and ε are the Lennard-Jones parameters. The separation and depth of the potential energy minimum between two similar molecules.

The simulated pressures along the supercritical isotherm using MD simulation with SPC model for water molecules were in good agreement with experimental pressures [73]. In our simulations, we used SPC model and the resulting charges and the angle of separation Q_1 (E), Q_2 (E), θ° where the same as the model had predicted and so gives credit to the type of water model we chose for the simulation.

3.9 Simulation Procedure

As mentioned, all simulations were carried out using Materials Studio v4.2.0.0 designed by Accelrys Software Inc. After the system was set up, it was minimized by the conjugate minimizer using Discover module. The convergence level which sets the level of accuracy required for all minimization methods was set at the medium level and the maximum iterations which specify the maximum number of iterations for a minimization calculation was set at its default value of 5,000. After minimization the amorphous cell is built. In this part, the number of the molecules determines the dimensions of the cell. After the cell is built another energy minimization is done with the same parameters as mentioned beforehand. Now, the system is ready to run the MD simulation using the Discover module. The ensemble was chosen as NVT and the temperature was set to the simulation temperature. The dynamics time which specifies the length of time of the simulations was 1,000ps. This also determines the number of steps. The time step set for each dynamic step was 1fs by default so the number of the steps during the whole simulation would be 1,000,000. During the simulation, a trajectory file was created which included information about the coordinates, velocities, energy components, pressure, etc. The data of the frames were written in the file every 5,000 steps. To control the temperature during the simulations a thermostat is used. The thermostats available were Velocity scale, Nose, Andersen and Berendsen. We used the Andresen thermostat. The collision ratio here which specifies the factor by which to multiply the collision period is 1. After the simulation was done, the macroscopic properties of interest can be gained by analyzing the simulated data.

Chapter 4

Results and Discussion

4.1 Testing the force field with supercritical data

First, we will examine if the force field used for the simulations (COMPASS) can be used for evaluating fluids at supercritical condition. Here, the calculated pressure is used for the validation. The pressure of supercritical fluids obtained from MD calculation was compared with those from the steam table. Pressure is a tensor. Each element of the pressure tensor is the force acting on the surface of an infinitesimal cubic volume that has edges parallel to the x, y, and z axes. The first subscript denotes the normal direction to the plane on which the force acts and the second one denotes the direction of the force.

Pressure is given by two components: (1) the momentum carried by the particles as they pass on the surface area and (2) the momentum transferred as a result of forces between interacting particles that recline on different sides of the surface.

$$P=\begin{bmatrix} P_{XX} & P_{XY} & P_{XZ} \\ P_{YX} & P_{YY} & P_{YZ} \\ P_{ZX} & P_{ZY} & P_{ZZ} \end{bmatrix} \quad (4.1)$$

In an isotropic situation, the pressure tensor is diagonal and the instantaneous hydrostatic pressure is calculated as:

$$P = \frac{1}{3}[P_{XX} + P_{YY} + P_{ZZ}] \quad (4.2)$$

By using the NVT ensemble, 100 water molecules were simulated in the supercritical region and below are the pressure results compared to experimental data. Each simulated pressure is the average of the last 20 steps of the simulation; the error bars are shown on top of each column.

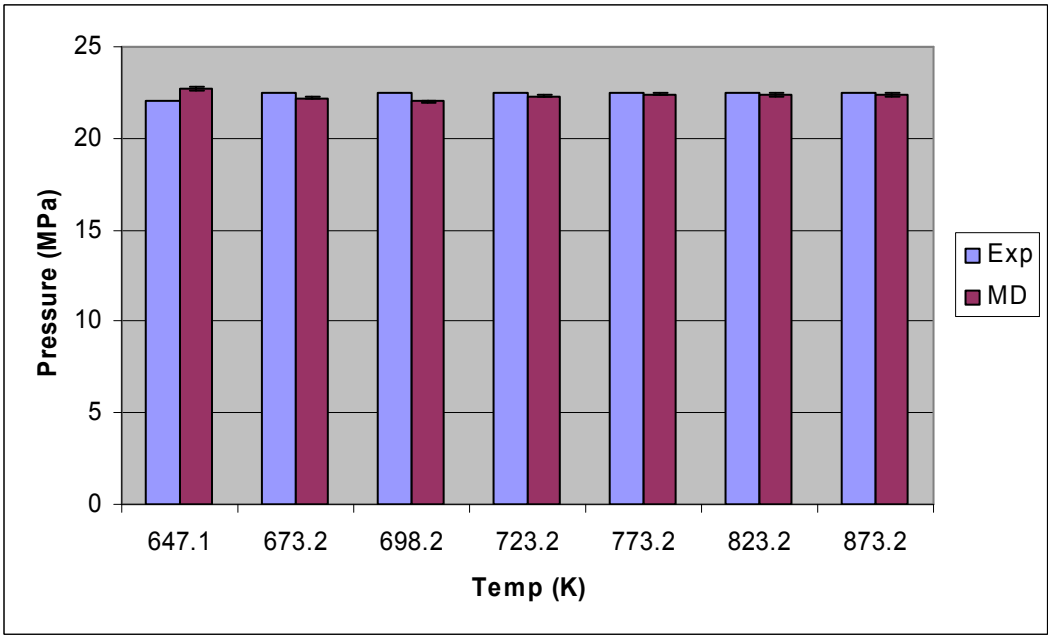

Figure 4-1 Pressure results, MD simulation vs. experiment

Carbon dioxide molecules were investigated as well, Since the density of supercritical carbon dioxide is very low the molecular dynamics simulations were run under two different densities: the former is 0.004 (mol cm^{-3}) and the latter 0.001. Experimental values for supercritical carbon dioxide come from Ref. [74].

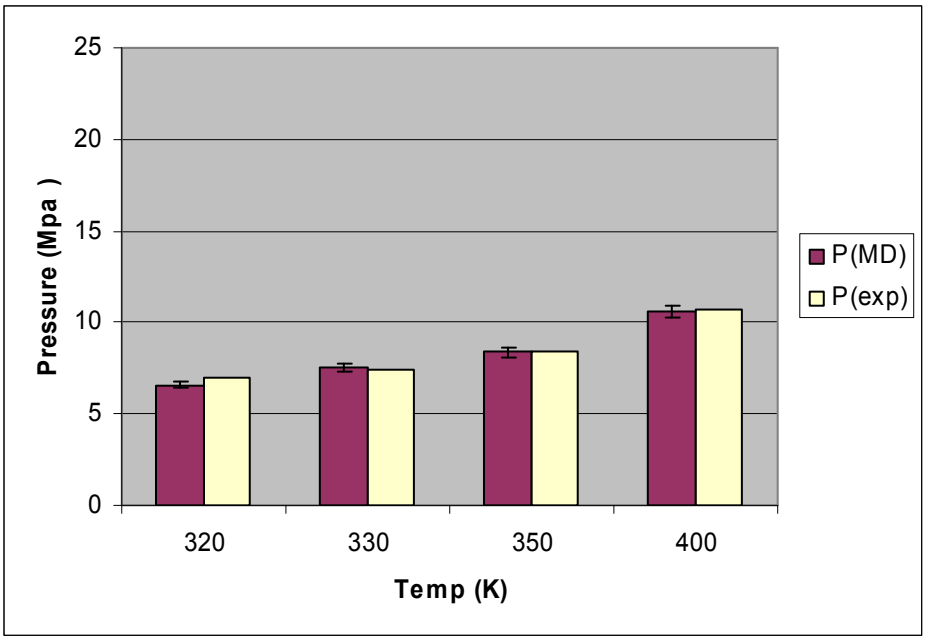

Figure 4-2 Pressure results for carbon dioxide, experiment vs. MD simulation at 0.004 (mol/cm^3)

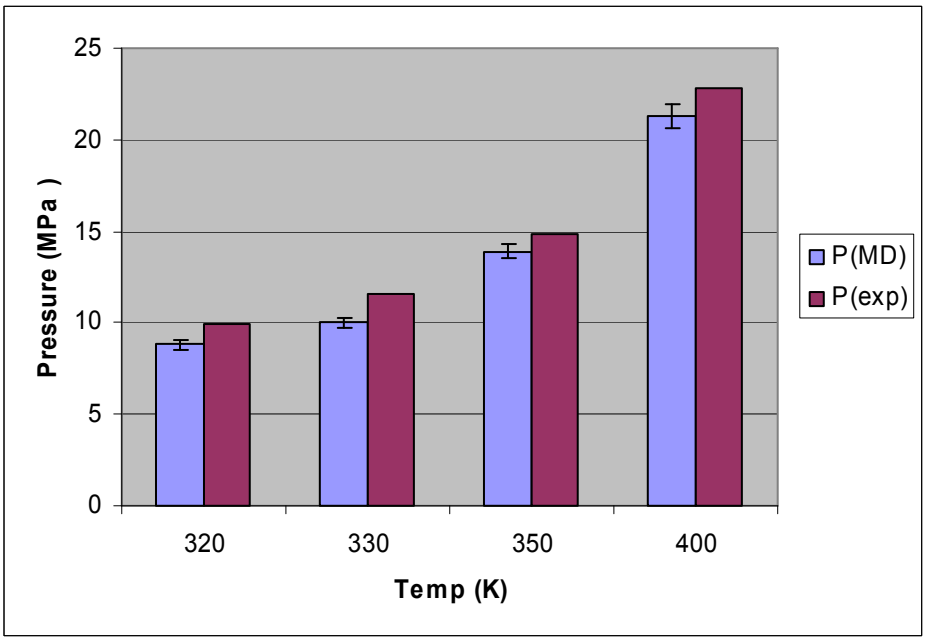

Figure 4-3 Pressure results for carbon dioxide, experiment vs. MD simulation at 0.001 (mol/cm^3)

In both cases, the simulated pressure of water and carbon dioxide match reasonably well with the experimental values, hence proves that the COMPASS force field is useful for investigating the supercritical regions of the two solvents.

4.2 System Size Dependence of Errors

It was noticed that the size of the errors of the computational results are dependent on the size of the amorphous cell used in the simulation. The cell size is altered by changing the number of the molecules in the simulation box from 5 to 400 molecules of water. Simulations were run in the NVT ensemble at 25 ^{0}C and 0.001 GPa. The results are shown in the graphs below (see Figure 4-4). There seems to be an optimum cell size for the simulations. The results were tested by other initial configurations and the same results were obtained. The optimum cell size is 21-23 angstroms. The reason for such an optimum point is not clear but it was viewed in literature that most of similar simulations were also run at this range of the cell. Therefore, all of our simulations were run around this cell size range for the sake of accuracy.

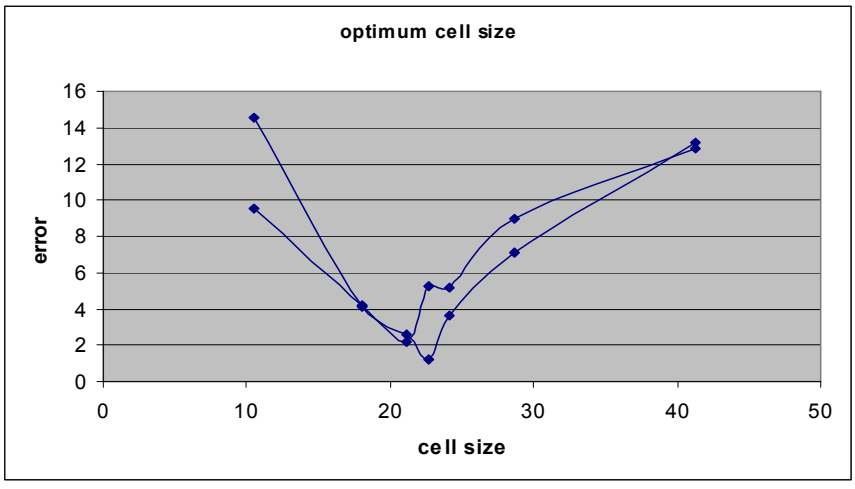

Figure 4-4 Optimum cell size for a sample simulation at 25 ^{0}C and 0.001 GPa, obtained from two initial configurations for each cell size

4.3 Solubility Parameters of Selected Organic Solvents at Room Temperature

Several organic solvents were simulated to gain their solubility parameters at ambient condition. One hundred molecules of each solvent were used to build the amorphous cell and the NVT ensemble was used for the simulations. The simulated results agree very well with the experimental values. Experimental numbers were obtained from the CRC handbook. Materials Studio uses the cohesive energy analysis to get the solubility parameter. The cohesive energy density (CED) calculation is performed on a series of structures obtained from the molecular dynamics trajectory. The energy of the system is recalculated for each structure without the periodic boundary condition to mimic the ideal gas situation .The CED is then calculated and reported in the output file together with the associated standard deviation, both in the form of a total CED and in terms of van der Waals and electrostatic components. In addition, a .tbl file is generated containing histograms of the cohesive energy densities and solubility parameters for all analyzed configurations. The results and the graph are shown as below:

Table 4-1 Calculated and experimental solubility parameters of four organic solvents and water at ambient temperature.

	Experiment	MD	%error
toluene	18.3	18.31	0.05
benzene	18.8	18.9	0.52
ethanol	26.2	26	0.77
n-hexane	14.9	4.84	0.40
water	47.9	47.67	0.48

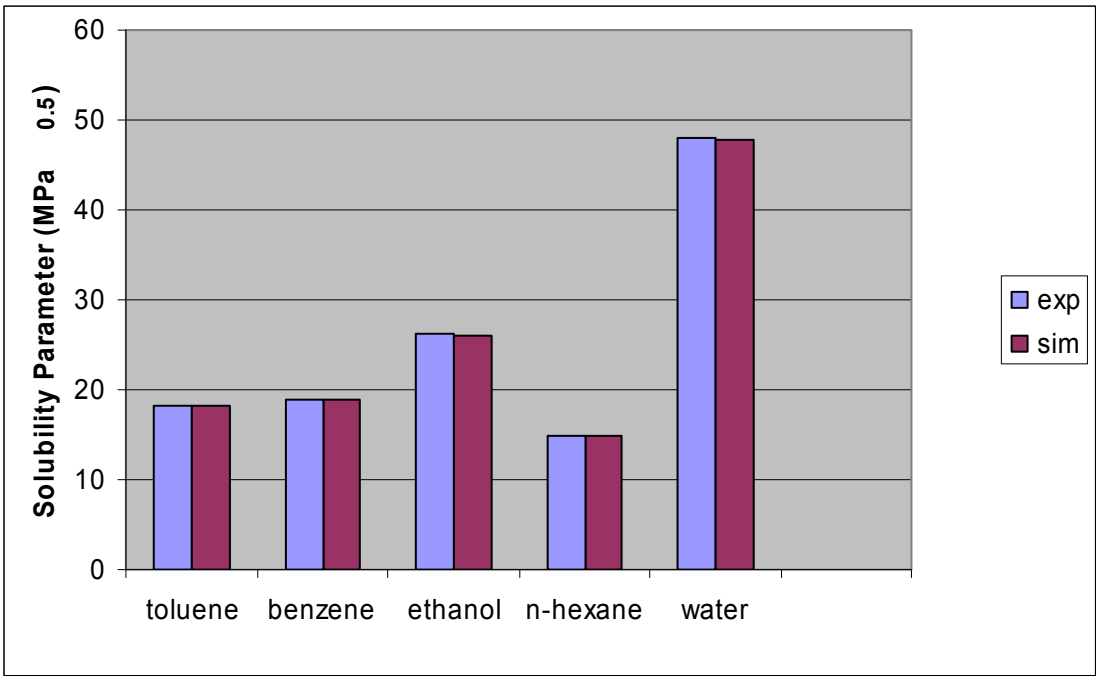

Figure 4-5 Solubility parameters for different solvents

4.4 Solubility Parameters of Selected Organic Solvents in the Supercritical Regions

Solubility parameters of 6 different solvents (water, ethanol benzene, toluene, n-hexane and CO_2) were calculated at ambient and supercritical conditions. The data pointing to the most left in each curve belongs to the solubility parameter of the solvent at ambient condition and the rest lie in the supercritical regions. Ranging from (647 to 873 K) at 22.5MPa. The solubility parameter of all solvents merges to approximately the same value (between 6 and 7 ($MPa^{0.5}$) as the temperature increases. Supercritical carbon dioxide seems to have slightly lower solubility parameter compared to other compounds.

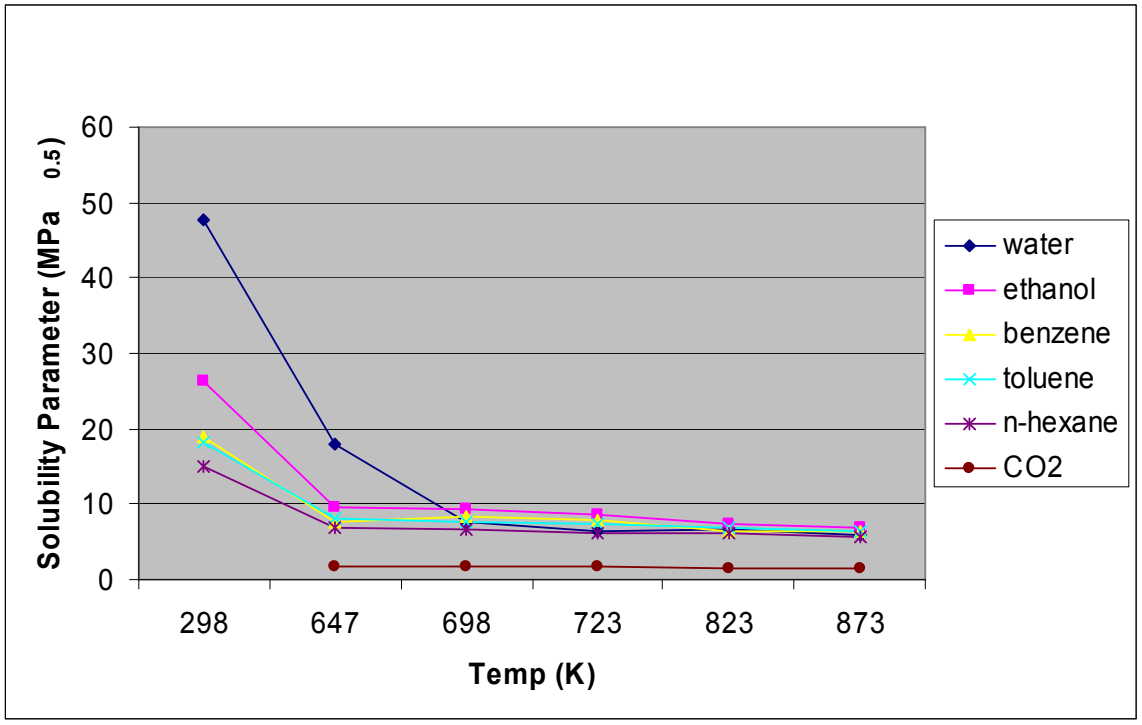

Figure 4-6 Solubility parameters for different solvents in SC regions

4.5 Solubility Parameters of Model Compounds at Ambient Temperature

Solubility parameters of the three model compounds were calculated with NVT ensemble and the results are in good agreement with experimental data. The asphaltene model compound shows greater deviation compared to the porphyrin model compounds. It is due to the branched structure of the asphaltene model compound; while the porphyrin structures are more symmetric.In our MD simulations the simulated solubility parameters have higher values than the experimental data. Other researches show asphaltene solubility parameter yields theoretical values that are lower than those reported experimentally of 19.5 $MPa^{0.5}$ and 20 $MPa^{0.5}$ [75]. Other authors found that the solubility parameter of asphaltenes is in the range 17.7-21.4 $MPa^{0.5}$ [76].

Table 4-2: Solubility parameters ($MPa^{0.5}$) for the 3 model compounds at 20 °C

	Experiment	MD	%error
H_2TPP	20	20.52	2.5
H_2OEP	19.9	20.34	2.1
PBP	20.6	23	10.4

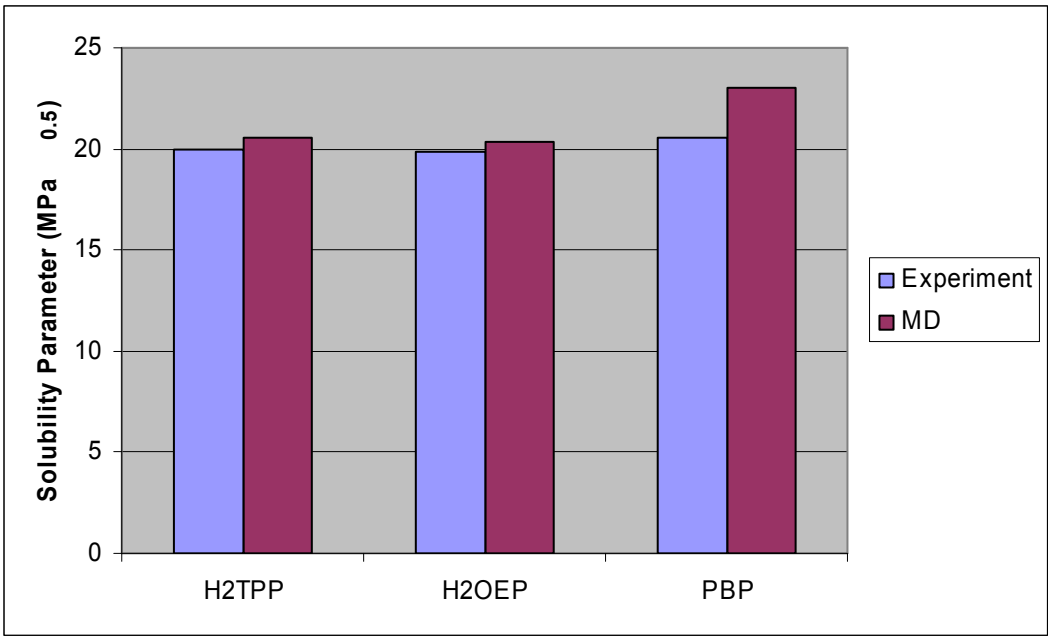

Figure 4-7 Solubility parameters for model compounds, Experiment vs. MD

4.6 Solubility Parameters of Model Compounds in the Supercritical Regions

Solubility parameters of the asphaltene model compounds also decrease as the temperature increases and get closer to the solubility parameters of carbon dioxide, water, and the selected organic solvents in their supercritical regions. Here, the pressure used was 22.5 MPa as well.

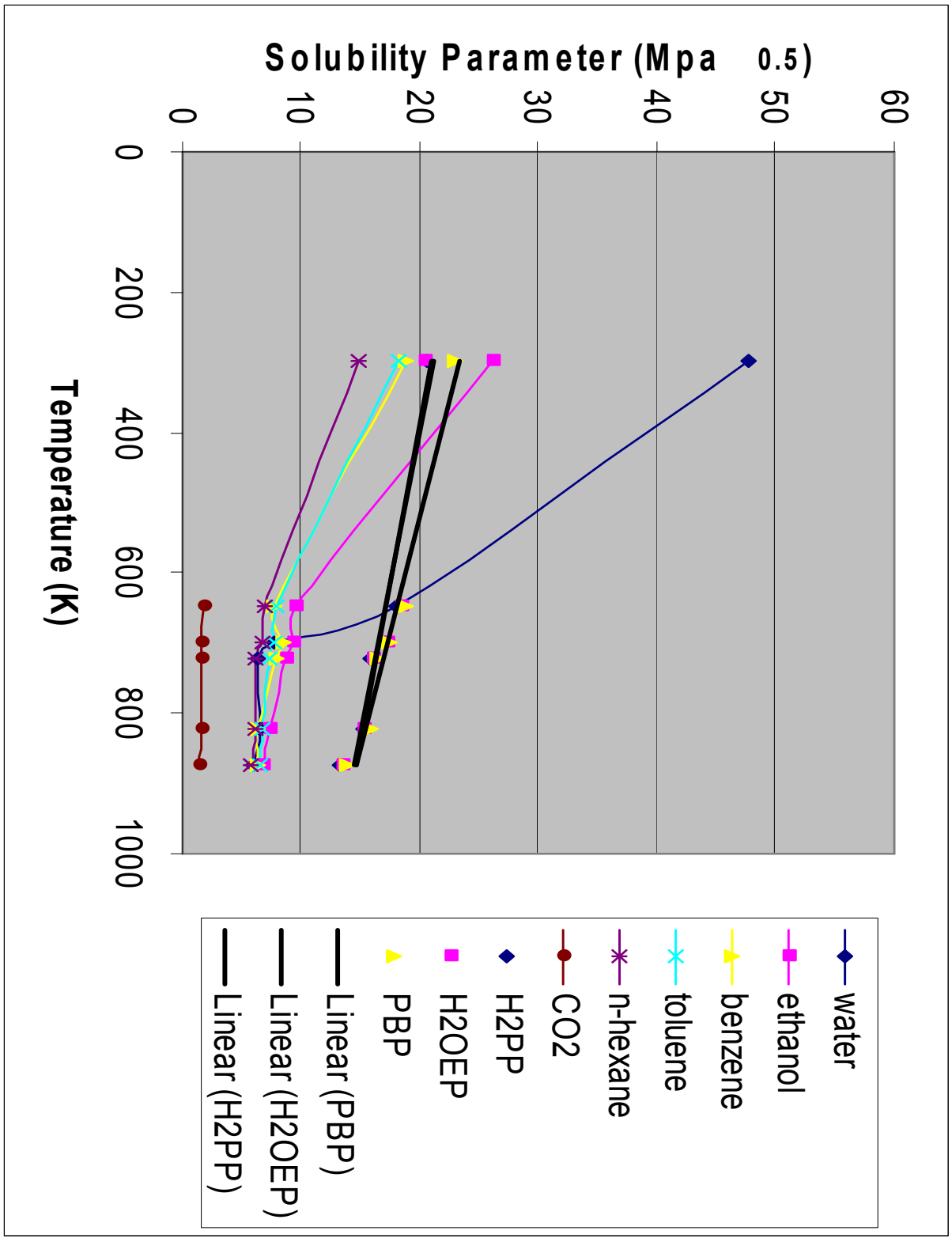

Figure 4-8 Solubility parameters of model compounds and supercritical fluids in SC regions

As the results for solubility parameters of the compounds in the supercritical regions show, Figure 4-8, it is almost impossible that model compounds can dissolve in supercritical carbon dioxide, since the difference between their solubility parameter is more than 4 $MPa^{0.5}$. It is worth noting that according to the Hildebrand solubility parameter theory, if the difference between the solubility parameters of two compounds is less than 4 $MPa^{0.5}$, they would dissolve into each other. It seems that at a pressure of 22.5 MPa, only water over a small range of temperature (~ 640-650 K) would dissolve the three model compounds.

4.7 Aggregation of H_2OEP Model Compounds in Supercritical Fluids

Results of MD simulations with binary mixtures containing model compounds and supercritical fluids support the previous results. In Figures 4-9, 4-10, 4-11 and 4-12, it is shown that the H_2OEP molecules stick together and form aggregates in supercritical fluids after 1,000 ps of MD annealing.the weight percet of model compound in the mixtures are 33%, 37%, 54% and 60% respectively. The simulations are run at 22.5 MPa and 700 K. This agrees with results gained from the solubility parameter approach reported in previous sections, the compounds do not dissolve in the chosen supercritical fluids. Also by comparing Figures 4-10 and 4-11 with Figures 4-12 and 4-13, it is evident that H_2OEP molecules tend to form more stable aggregates in supercritical carbon dioxide than in supercritical water which also agrees with results in section 4.4 that the solubility parameter of supercritical carbon dioxide is lower than that of supercritical water.

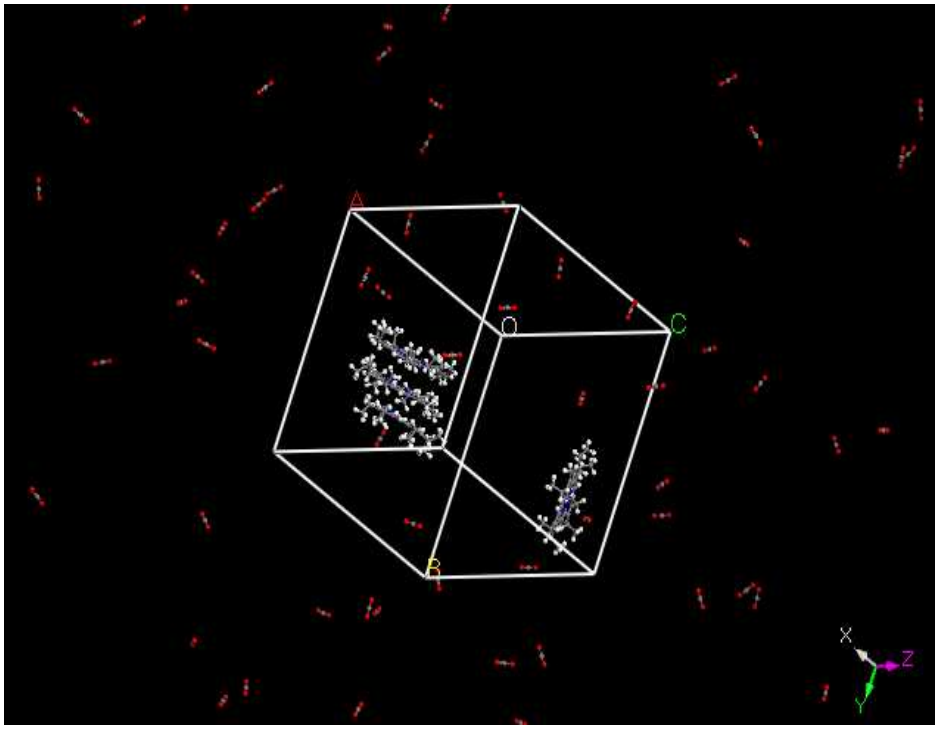

Figure 4-9 Mixture of five H_2OEP and one hundred CO_2 molecules in the SC region

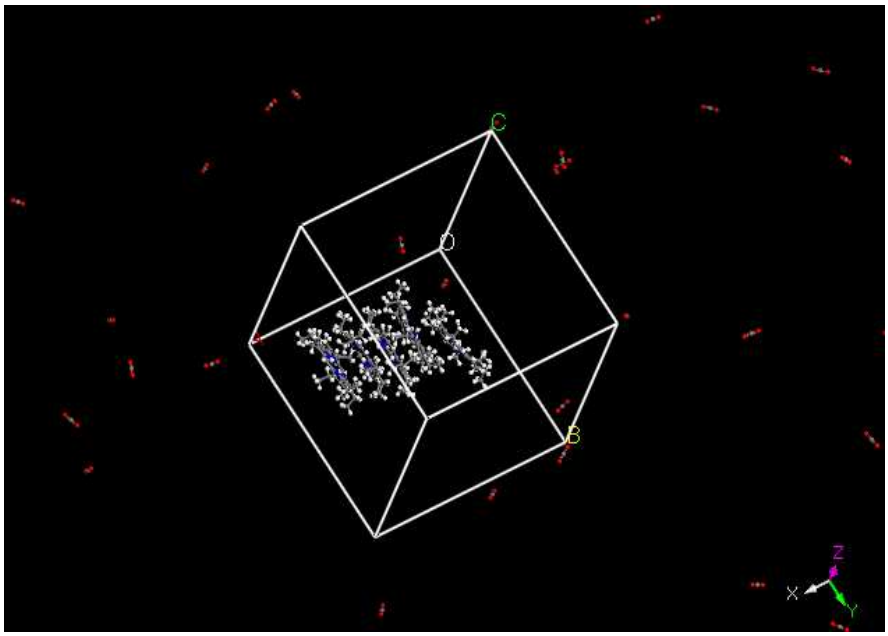

Figure 4-10 Mixture of four H_2 OEP and one hundred CO_2 molecules in the SC region

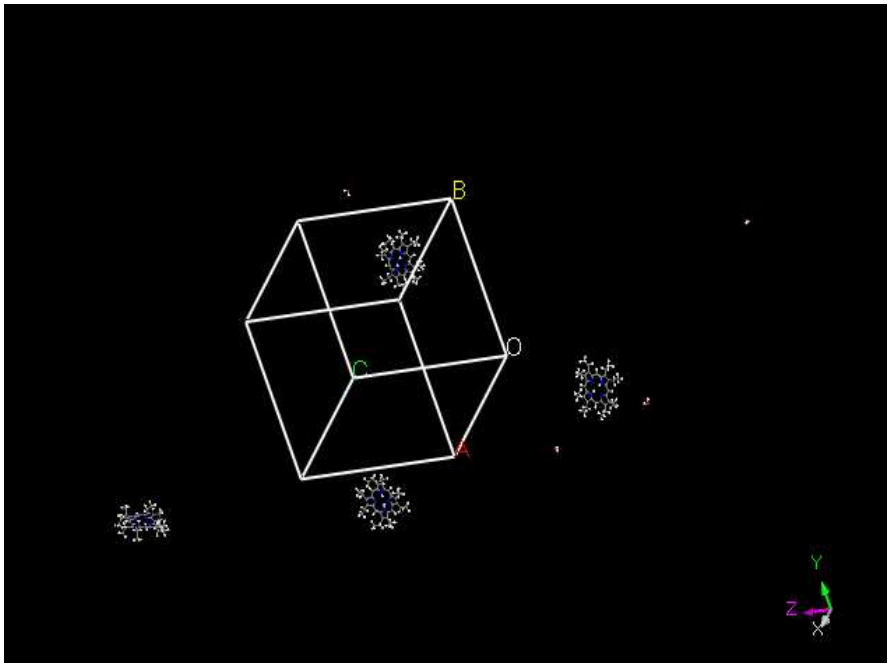

Figure 4-11 Mixture of four H_2 OEP and one hundred H_2O molecules in the SC region

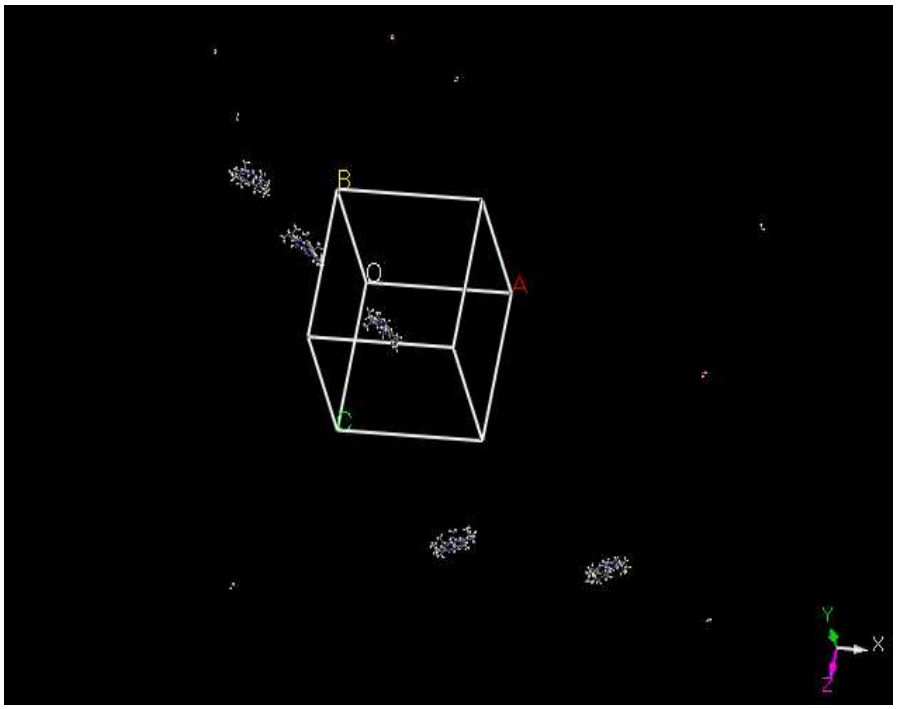

Figure 4-13 Mixture of four H_2 OEP and one hundred H_2O molecules in the SC region

Chapter 5

Conclusion and Future work

5.1 Conclusion

The main motivation behind this thesis was to study solubility properties of porphyrin and asphaltene model compounds in supercritical fluids. Water, carbon dioxide and several selected organic solvents in their supercritical states were studied. Three model compounds were used: Meso-tetraphenyl porphyrin (H_2TPP) and Octaethyl porphyrin (H_2OEP) are the porphyrin model compounds and; 4'-Bis-(2-pyren-1-yl-ethyl)-[2, 2'] bipyridinyl (PBP) is the asphaltene model compound.

First, the viability of using the COMPASS force field for supercritical calculation was tested by calculating supercritical pressure in NVT ensemble for water and carbon dioxide and comparing the results with experimental data they agree favorably.

Miscibility prediction based on a solubility parameter approach was used during this study. The solubility parameters of selected organic solvents and the model compounds were calculated at ambient pressure and temperature which compared favorably with experiment. The method to obtain the experimental values for model compounds was described in the text.

The relevancy of the concept of solubility parameter to supercritical fluid was reviewed. It was noticed that the computed solubility parameters of water and the selected organic solvents converge at elevated temperatures while the solubility parameter of carbon dioxide is less than the rest of the solvents in their supercritical regions.

The solubility parameters of all three model compounds decreased by increasing temperature in their respected supercritical regions; the differences between the solubility parameters of the model compounds and the supercritical carbon dioxide were large indicating that they don't dissolve into each other; however all three model compounds dissolve into supercritical water at it close to its critical point, 22.5 MPa and 640-650 MPa.

Finally, the validity of previous results is also proved using simulation of mixtures of model compounds and supercritical fluids. The simulations show that H_2OEP forms aggregates in both supercritical water and supercritical carbon dioxide in agreement with solubility parameter approach. The aggregates in supercritical carbon dioxide are more stable than in supercritical water which shows the solubility power of supercritical carbon dioxide is less than supercritical water, also in agreement with the solubility parameter approach.

5.2 Future Work

As for future work, the association of the model compound molecules in binary mixtures containing supercritical fluids should be carried out to confirm the prediction from the

solubility parameter approach. Also, it is well established that a small amount of polar cosolvents can significantly increase the interaction between supercritical fluids and polar low-molar mass solutes, based on the experimental results [77, 78] and molecular simulation [79]. The impact of addition of a cosolvent to supercritical carbon dioxide on its solubility parameter can be a topic of interest for future work as well.

For practical purposes, the fact that models compounds do not dissolve in supercritical carbon dioxide, means they would precipitate in it; hence supercritical carbon dioxide can be used to isolate asphaltenes from petroleum and its heavy residues. The method compromises the dissolution of a test sample in supercritical carbon dioxide or in a mixture of hydrocarbon solvent with supercritical carbon dioxide and the subsequent precipitation of asphaltenes under the carbon dioxide supercritical conditions.

References:

1. L. T. Taylor, “Supercritical Extraction”, John Wiley & Sons: New York, 1996.
2. M. A. McHugh, V. J. Krukonis, “Supercritical Fluid Extraction: Principles and Practice” 2nd ed. Butterworth: Stoneham, MA, 1994.
3. G. Parkinson, E. Johnson, “Supercritical Processes Win CPI Acceptance”. Chem. Eng. (1989) 37.
4. G. G. Hoyer, “Extraction with Supercritical Fluids: Why, How, and so What?” CHEMTECH. 1985(440).
5. D. F. Williams, “Extraction with Supercritical Gases”. Chem. Eng. Sci. 36 (1981) 1769.
6. J. G. Speight, “the Chemistry and Technology of Petroleum”, 2nd ed.; Marcel Dekker: New York, 1991.
7. A. Sunol, H. Beyer, “Mechanism of Supercritical Extraction of Coal”. Ind. Eng. Chem. Res. 29(1990) 842.
8. J. R. Kershaw, L. J. Bagnell, “Extraction of Australian Coals with Supercritical Aqueous Solvents in Supercritical Fluids” Chemical and Engineering Principles and Applications; American Chemical Society: Washington, D.C., 1987.
9. S. K. Kesavan, A. Ghosh, M. E. Polasky, V. Parameswaran, S. Lee, “Supercritical Extraction of Stuart Oil Shale”. Fuel Sci. Technol. 6(1998) 505.
10. J. Triday, J. M. Smith, “Dynamic Behaviour of Supercritical Extraction of Kerogen from Shale”. AIChE J. 34(1998) 658.
11. K. D. Bartle, A. Erdem-Senetalar, E. Kadioglu, M. Tolay,”Sub-Critical and Super-Critical Solvent Extraction of the Avgamasya Asphaltite of South Eastern Turkey”. In Characterisation of Heavy Crude Oils and Petroleum Residues: Symposium International. Lyon, France, June, (1984) 217.
12. M. D. Deo, J. Hwang, F. V. “Hanson, Supercritical Fluid Extraction of a Crude Oil, Bitumen-Derived Liquid and Bitumen by Carbon Dioxide and Propane”. Fuel. 71(1992)1519.
13. M. Subramanian, F. V. “Hanson, Supercritical Fluid Extraction of Bitumens from Utah Oil Sands”. Fuel Process. Technol. 55(1998) 35.
14. H. J. Oschmann, U. Prahl, D. Severin, “Separation of Paraffin from Crude Oil by Supercritical Fluid Extraction”. Pet. Sci. Technol. 16(1998) 133.
15. J. Cheng, Y. Fan, Y. Zhan, “Supercritical Propane Fractionation of Wax-Bearing Residue”. Sep. Sci. Technol. 29(1994) 1779.

16. K. H. Chung, C. Xu, Y. Hu, R. Wang, “Supercritical Fluid Extraction Cuts Deep into the Bottom of the Barrel”. 46th Canadian Chemical Engineering Conference, Kingston, Canada, 1996.

17. G. B. Lim, R. P. Kry, B. C. Harder, K. N. Jha, “Cyclic Stimulation of Cold Lake Oil Sand with Supercritical Ethane”. International Heavy Oil Symposium, Society of Petroleum Engineers, Calgary, Canada, 1995.

18. M. Gray, J. Masliyah, Z. Zou, “Physics in the oilsands of Alberta”, Physics Today, 62 (2009) 31-35.

19. M. Fox, "Venezuela increases taxes on oil companies in Orinoco oil belt", Venezuelaanalysis, http://venezuelanalysis.com/news/1735 (accessed August 16, 2010).

20. National Energy Board of Canada, “Canadian Energy Overview 2007". (accessed May 16, 2007).

21. Wikipedia contributors, "Hildebrand solubility parameter," Wikipedia, the Free Encyclopedia,http://en.wikipedia.org/w/index.php?title=Hildebrand_solubility_parameter&oldid=373948322 (accessed August 17, 2010).

22. J.M. Smith, H. Van Ness, M.M. Abbott, Introduction to Chemical Engineering Thermodynamics, 5th ed.McGraw-Hill, New York, 1996.

23. J. Chrastil, Solubility of solids and liquids in supercritical gases, J. Phys. Chem. 86 (1982) 3016.

24. C.I. Lu¨ tge, A. Reiss, S. Schleussinger, S. Schultz, Modeling the extraction of perylene from spiked soil material by dense Carbon dioxide, J. Supercrit. Fluids 7 (1994) 265.

25. J.M. Wong, R.S. Pearlman, K.P. Johnston, Supercritical fluid mixtures: prediction of the phase behavior, J. Phys. Chem. 89 (1985) 2671.

26. K.P. Johnston, D.G. Peck, S. Kim, Modeling mixtures: how predictive is it? Ind. Eng. Chem. Res. 28 (1989) 1116.

27. J.F. Brennecke, C.A. Eckert, Phase equilibria for supercrit-ical fluid process design, AIChE J. 35 (1989) 1409.

28. J.C. Giddings, M.N. Myers, L. McLaren, R.A. Keller, High-pressure gas chromatography of nonvolatile species, Science 162 (1968) 67–73.

29. J.C. Giddings, M.N. Myers, J.W. King, Dense gas chromatography at pressures to 2000 atmospheres, J. Chromatogr. Sci. 7 (1969) 276–283.

30. J.W. King, Supercritical fluid extraction of polymers and solvents: utilization of the solubility parameter concept, Polym. Mater. Sci. Eng. 51(1984) 707–712.

31. M.L. Riekkola, P. Manninen, Supercritical-fluid extraction as an alternative sample preparation method, Trends Anal. Chem. 12 (1993) 108–114.

32. Y. Ikushima, T. Goto, M. Arai, Modified solubility parameter as an index to correlate the solubility in supercritical fluids, Bull. Chem. Soc. Jpn.60 (1987) 4145–4147.

33. S.R. Allada, Solubility parameters of supercritical fluids, Ind. Eng. Chem. Proc. Des. Dev. 23 (1984) 344–348.

34. C. Panayiotou, Solubility parameter revisited: an equation-of-state approach for its estimation, Fluid Phase Equilib. 131 (1997) 21–35.

35. S. Goldman, C.G. Gray, W. Li, B. Tomberli, C.G. Joslin, Predicting Solubilities in Supercritical Fluids. J. Phys. Chem. 100 (1996) 7246−7249.

36. W. Li, B. Tomberli, C.G. Joslin, Solubilities in supercritical fluids, J. Phys. Chem. 100 (1996) 7246–7249.

37. E. Rogel, Physicochemical and Engineering Aspects 104 (1995) 85-93.

38. A.F.M. Barton, CRC Handbook of Solubility Parameters and Other Cohesion.

39. L. Gui-wu1, L. Ying-feng1, S. Hui2, Y. Ying-hui1, W. Chun-lei, Petrol. Explore. Develop. 35(2008) 67-72.

40. O. C. Mullins, Springer, 46 (2007) 700.

41. Wikipedia contributors, "Asphaltene," *Wikipedia, the Free Encyclopedia,* http://en.wikipedia.org/w/index.php?title=Asphaltene&oldid=358168956 (accessed August 12, 2010).

42. K.A. ferworn, W.Y. Svrcek and A.K. Mehrotra, Ind. Eng. Chem. Res. 32(1993) 955.

43. A. Bhardway and D. hartland, Ind. Eng. Chem. Res. 33 (1994) 1271.

44. J.G. Speight, in L.B Ebert (Ed), Polynuclear aromatic compounds, Adv. Chem. Ser. (1998) 217.

45. M.M.F. Al-jarrah and A.H. Al-Dujaili, Fuel Sci. Technol. Int. 7(1994) 1324.

46. M.M. Boduszynski, Energy Fuels, 2(1988) 597.

47. K.J. Leontaritis and G.A Mansoori, Int. J. Pet.Sci. Eng, 2 (1989) 1.

48. M.M. Boduszynski, Energy Fuels, 1 (1987) 2.

49. J.G. Speight and S.E. Moschopedis. Preprints Am. Chem. Soc. Div. Fuel. Chem, 23 (1979) 1910.

50. A.F.M.Barton. Handbook of solubility parameters and other cohesion parameters, CRC press, Inc. USA, 1983.

51. S.I. Andersen, J.G. Speight, J. Petrol. Sci. Eng. 22 (1999) 53-66.

52. G.A. Mansoori, J. Petrol. Sci. Eng. 17 (1997) 101-111.

53. H.C.A. Brandt, E.M. Hendriks, M.A.J. Michels, F. Visser, J. Phys. Chem. 99(1995) 10430-10432.

54. E. Rogel, Colloid Surf.A 104 (1995) 85-93.

55. J.Murgich, J.Rodriguez, Y. Aray, Energy. Fuel 10 (1996) 68-76.

56. G.W. Zajac, N.K. Sethi, J.T. Joseph, Scanning Microsc. 8 (1994) 463-470.

57. B. J. Alder and T. E. Wainwright, J. Chem. Phys, (1957) 1208.

58. D. Chandler, "Introduction to Modern Statistical Mechanics", (1987, Oxford University Press).

59. M. J. Gillan, Phys. Scripta, 362 (1991).

60. P. J. D. Lindan and M. J. Gillan, J. Phys.: Condens. Matter 3, 3929 (1991).

61. M. P. Allen, D. J. Tildesely, "Computer Simulation Liquids"(Oxford University Press, 1987).

62. J. M. Haile, "Molecular dynamics simulation: elementary methods", (Wiley, 1992).

63. F. Reinitzer Montash. Chem. 9 (1888) 421.

64. C. E. Fairhurst, S. Fuller, J. Gray, M. C. Holmes, G. J. T. Wiley-VCH 3(1998) 341.

65. C. Zannoni *J.* Mater. Chem. 11 (2001) 2637.

66. T. C. Lubensky Solid State Comm. 102 (1997) 187.

67. P. A. Lebwohl and G. Lasher Phys. Rev. *A* 6, (1972) 426.

68. M. A. Glaser, "Liquid Atomistic Simulation and Modeling of Smectic Crystals in Advances in the Computer Simulation of Liquid Crystals", editors P. Pasini and C. Zannoni Kluwer, Dordecht (2000).

69. K.-J. Lee, G.-H. Hsuie, J.-L. Wu and J.-H. Chen *Liq. Cryst.* 26 (1999) 46.

70. L. Verlet Phys. Rev. 159 (1967) 98.

71. D. J. Evans and G. P. Morris Phys. Lett 98A, (1983) 433.

72. J. L. Finney, "The water molecule and its interactions: the interaction between theory, modeling and experiment", J. Mol. Liq. 90 (2001) 303-312.

73. T. I. Mizan, P. E. Savage, R. M. Ziff, J. Phys.Chem.,1994**,** 98 (49).

74. S. Angus, B. Armstrong and K.M. deReuck, “Carbon dioxide”, international thermodynamic tables of the fluid state, 3 (1973).

75. N.E Burke, R.E.Hobbs and S.F.Kashov, J. Pet. Technol, November, 1990, 1440.

76. H. Lian, J.R. Lin, T.F. Yen, Fuel, 73 (1994) 423.

77. C.R. Yonker and R.D. Smith, J. Phy. Chem., 92 (1988) 2374.

78. 2. B.L. Knutson, S.R. Sherman, K.L. Bennett, C.L. Liotta, and C.A. Eckert, Ind. Eng. Chem. Res., 36 (1997) 854.

79. I.B. Petsche, P.G. Debenedetti, J. Chem. Phys., 91 (1989) 7075.